Human cardiosphere-derived stromal cells exposed to SARS-CoV-2 evolve into hyper-inflammatory/*pro*-fibrotic phenotype and produce infective viral particles depending on the levels of ACE2 receptor expression

Alessandra Amendola[1,*], Gloria Garoffolo[2,3,*], Paola Songia[2], Roberta Nardacci[1], Silvia Ferrari[2,4], Giacomo Bernava[2], Paola Canzano[2], Veronika Myasoedova[2], Francesca Colavita[1], Concetta Castilletti[1], Giuseppe Sberna[1], Maria Rosaria Capobianchi[1], Mauro Piacentini[5], Marco Agrifoglio[2,6], Gualtiero I. Colombo[2], Paolo Poggio[2], and Maurizio Pesce[2,§]

1. Istituto Nazionale Malattie Infettive, Lazzaro Spallanzani; IRCCS, Rome, Italy

2. Centro Cardiologico Monzino; IRCCS, Milan, Italy

3. PhD Program in Translational and Molecular Medicine - DIMET; Università di Milano - Bicocca, Italy

4. PhD Program in Translational Medicine; Università degli studi di Pavia, Italy

5. Università degli studi di Roma 'Tor Vergata'; Rome, Italy

6. Università degli studi di Milano; Milan, Italy

*These Authors contributed equally to this work

§ Author for correspondence: Maurizio Pesce, PhD; Unità di Ingegneria Tissutale Cardiovascolare, Centro Cardiologico Monzino, IRCCS, Via C. Parea, 4, I-20138, Milano, Italy

Keywords

SARS-CoV-2; cardiac stromal cells; ACE2; infection; inflammation; fibrosis

Running title

Human cardiac stromal cells infection by SARS-CoV-2

Abstract

Aims - Patients with severe respiratory syndrome caused by SARS-CoV-2 undergo cardiac complications due to hyper-inflammatory conditions. Although the presence of the virus has been detected in the myocardium of infected patients, and infection of induced pluripotent cells-derived cardiomyocytes has been demonstrated, the reported expression of ACE2 in cardiac stromal cells suggests that SARS-CoV-2 may determine cardiac injury by sustaining productive infection and increasing inflammation.

Methods and Results - We analyzed expression of ACE2 receptor in primary human cardiac stromal cells derived from cardiospheres, using proteomics and transcriptomics before exposing them to SARS-CoV-2 *in vitro*. Using conventional and high sensitivity PCR methods, we measured virus release in the cellular supernatants and monitored the intracellular viral bioprocessing. We performed high-resolution imaging to show the sites of intracellular viral production and demonstrated the presence of viral particles in the cells with electron microscopy. We finally used RT-qPCR assays to detect genes linked to innate immunity and fibrotic pathways coherently regulated in cells after exposure to the virus.

Conclusions - Our findings indicate that cardiac stromal cells are susceptible to SARS-CoV-2 infection and produce variable viral yields depending on the extent of cellular ACE2 receptor expression. Interestingly, these cells also evolved toward hyper-inflammatory/pro-fibrotic phenotypes independently of ACE2 levels. Thus, SARS-CoV-2 infection of myocardial stromal cells could be involved in cardiac injury, and explain the high number of complications observed in severe cases of COVID-19.

Translational Perspective

In the present investigation, we provide evidence that human cardiac stromal cells, a major component of the non-contractile cellular fraction in the heart can be infected by SARS-CoV-2 *in vitro*, in direct relationship to the extent of ACE2 receptor expression. Our work also suggests that these cells, when exposed to the virus, can evolve toward inflammatory and fibrotic phenotypes independently of ACE2. In addition to describing a novel cellular target of SARS-CoV-2 in the human heart, our study generates new hypothesis on potential mechanisms underlying cardiac complications observed in COVID-19 patients.

1. Introduction

Since the beginning of the SARS-CoV-2 pandemic outbreak, a relatively high incidence of cardiac complications have been reported[1, 2]. These range from elevation of cardiac damage markers such as circulating troponin and BNP[3, 4], to cardiac arrest[5], cardiogenic shock[6], myocarditis[7] and heart failure[8]. The susceptibility of the myocardial tissue to SARS-CoV-2 infection[6, 9] has been inferred based on the expression of the Angiotensin-Converting Enzyme-2 (ACE2) receptor in various cardiac cell types[10, 11], and the evidence that the virus interacts with this receptor *via* the Spike (S) protein, as a main cellular docking/internalization site[12].

In an attempt to explain the cardiac complications observed in patients with COVID-19, experimental studies have tried to assess the direct susceptibility of endothelial cells[13, 14] and induced pluripotent cells (iPSCs)-derived cardiac myocytes[15, 16] to SARS-CoV-2 infection, with contrasting results. Furthermore, individual variations in the level of ACE2 mRNA expression have been reported by single-cell RNA sequencing in human myocardial cells, including cardiac fibroblasts[11], thus providing a rationale for the possible involvement of these cells in the cardiac damage observed in patients with COVID-19. Cardiac stromal cells (cSt-Cs), often also referred to as cardiac fibroblasts[17], are non-contractile myocardial cells that fulfill an important accessory function in the heart, *i.e.* the renewal of the extracellular matrix and maintenance of myocardium structural integrity. These cells can be derived in culture using different isolation methods and express a variety of mesenchymal and/or fibroblast markers, likely related to different origins and maturity stages[18]. Under pathologic conditions, e.g. in response to ischemia, cSt-Cs can acquire *pro*-inflammatory/*pro*-fibrotic phenotypes, and participate in cardiac inflammation and fibrosis[19-22].

Based on these evidences we hypothesized that cardiac complications observed in COVID-19 could be due, at least in part, to the combined effects of direct infection and *pro*-inflammatory/*pro*-fibrotic conversion of cardiac stromal cells. To address this possibility, we analyzed the effects of the SARS-CoV-2 virus on cSt-Cs derived from cardiospheres[23] *in vitro*, in correlation to the extent of ACE2 receptor expression.

2. Methods

2.1. Ethics

The use of human cells for *in vitro* experiments was approved by the local ethical committee (approval date: 19 May 2012 and subsequent renewal on 16 May 2016) and has been performed in conformity with the principles

of the declaration of Helsinki. Patients gave their written consent to donate small fragments of right atrial appendage before routine coronary bypass grafting interventions. Collection of material occurred before the beginning of the SARS-CoV-2 pandemic outbreak. Experiments performed with SARS-CoV-2 *in vitro* did not require specific ethical authorization according to a specific instruction ("Data processing in clinical trials and medical research in the context of the COVID-19 health emergency" - article 3), published by the Italian Data Protection Authority to rule the use of patients material in case of experimental studies on COVID-19. See https://www.garanteprivacy.it/temi/coronavirus/faq#English for more information.

2.2. Derivation of cardiac stromal cells.

Cardiac stromal cells were derived using the 'cardiosphere' method[23]. Briefly, small fragments of the cardiac tissue were let to attach onto the bottom of tissue culture dishes, until an outgrowth of cells was achieved. Following a mild digestion with Trypsin, cells were recovered and sub-cultured onto Poly-D-Lysine coated dishes for cardiosphere formation. Cardiosphere-derived cells were obtained from mature cardiospheres, typically after 3-5 wks of culture by digestion of the cell aggregates and expansion in fibronectin-coated dishes. Cells were used for experiments at passage 2-3 after derivation from cardiospheres, and characterization with RT-qPCR, Western analysis and flow cytometry for assessment of ACE2 receptor expression (see Supplementary Information).

2.3. Design of SARS-CoV-2 infection experiments.

After thawing, three cSt-Cs lines were plated at a 60% confluence in 6-well culture plates and exposed to variable amounts (0.1, 1, 10 multiplicity of infection, MOI) of SARS-CoV-2 isolates in a biosafety level (BSL) 3 facility[24] in technical quadruplicates. After 2, 24, and 72 hours, cells underwent RNA extraction and immunofluorescence staining, while culture supernatants were collected, as described in Supplementary Information.

2.4. Detection of cSt-Cs phenotype after exposure to SARS-CoV- in vitro.

To assess changes in cSt-Cs phenotype after exposure to SARS-CoV-2 *in vitro*, RT-qPCR assays were conducted on total RNA extracted from cells exposed at each viral concentration and time points. In addition, immunofluorescence staining for SARS-CoV-2 in combination with other cellular markers and transmission electron microscopy were performed. Details of the RNA analysis and microscopy methods are provided in the Supplementary Information.

3. Results

3.1. Variability in expression of ACE2 receptor in human cSt-Cs

To assess the expression of ACE2 receptor in cardiac stroma cells, we analyzed the levels of ACE2 protein expressed in 10 lines of human cardiospheres-derived cSt-Cs available to our laboratory (see Supplementary Information for the methodology of isolation and expansion)[23]. **Figure 1A** shows the results of the ACE2 expression in the cSt-Cs by Western Blotting and RT-qPCR. A relatively high variability in the expression of the receptor was observed (**Figure 1A**), with no apparent relationship with demographic characteristics (i.e. age), risk conditions (e.g. dyslipidemia, hypertension) or medication (e.g. anti-hypertensive treatment) (**Table S1**). On the other hand, ACE2 protein expression was highly correlated with the levels of *ACE2* gene transcription, as verified by a linear regression analysis of the RNA/Protein expression data (**Figure 1A**). This indicates that the control of *ACE2* expression in cST-Cs occurs at a transcriptional level. In keeping with results obtained with other primary human-derived mesenchymal cell lines, TMPRSS2 the other major receptor facilitating SARS-CoV-2 infection[25] was not expressed by cSt-Cs (data not shown).

3.2. ACE2 dependency of human cSt-Cs infection in vitro

To classify the cells for ACE2 expression, we grouped the cSt-Cs into three discrete classes (high, medium and low expression) based on the distribution of both the ACE2 protein normalized expression level (by Western Blot) and of the $2^{-\Delta Ct}$ gene expression data (by RT-qPCR) data, using K-means clustering (**Figure S1**). For the remaining experiments, we chose three cSt-Cs lines obtained from donors with the most similar demographic characteristics (age, sex) and risk profile (diabetes, hypertension), one for each ACE2 expression classes. They are indicated as ACE2 'Hi', 'Mid' and 'Lo' in the rest of the experiments. The main characteristics of the cell donors are present in **Table S1**. The three cell lines were tested for expression of cardiac fibroblast/mesenchymal markers[26]. As shown in **Figure 1B**, the expression of CD29 and CD44 was very similar, while a relatively higher variability was observed for the expression of CD90 and CD105, typical markers of cardiac-resident mesenchymal cells[27]. This variability, however, remained within the limits of the general variation in expression of mesenchymal markers in cells amplified from all donors (**Figure 1B**). All these cells, finally, did not express endothelial markers CD31 and CD144 (**Figure 1B)**, excluding contamination by endothelial cells. To assess the susceptibility to SARS-CoV-2 infection, we exposed them to increasing amounts (multiplicity of infection, MOI: 0.1, 1, and 10; see **Supplementary information** for details) of SARS-CoV-2 isolates[24], and monitored the appearance of cytopathic effects, from two to 72 hours post-infection. Visual

inspection of the cells revealed potential differences according to the infection rate, with clear signs of cytopathic effects in ACE2 Hi cells already at two hours after the viral absorption, and consisting of cell rounding and wrinkling, cytoplasmic volume reduction, and detachment (**Figure 1C**). These effects were noticeable at a lower extent, in 'Mid' cells, and undetectable in ACE2 'Lo' cSt-Cs, even at 72 hours post-infection (data not shown). In order to monitor the viral yield in the culture supernatants of the three cell lines, we performed RT-qPCR to detect SARS-CoV-2 *Spike* and *ORF* coding RNAs in the collected culture medium at 2, 24 and 72 hours post-infection. Analysis of the Ct values showed a clear trend of the three cell lines to release increasing levels of the virus in the supernatant at 24 and 72 hours compared to those released 2 hours post infection at all the MOI (**Figure 1D**). These trends were, however, not significant, likely due to the differences in the response of the cells in relationship with the variable expression of ACE2. In fact, plotting the Ct values trends of each of the cell lines individually (**Figure 1E**), revealed that ACE2 'Lo' cells did not release the virus in the supernatant, as shown by the almost flat Ct curve as a function of time at all the considered virus concentrations. By contrast, 'Mid' and 'Hi' cells exhibited an increase in the curve of viral RNAs amplification, evident for 'Mid' cells at 72 hours at 10 MOI, and for 'Hi' cells at 24 and 72 hours at all the MOIs, suggesting viral production. To confirm these data more quantitatively, we assessed the copy number of the virus in the supernatant using a digital-PCR (dPCR) amplification protocol, using primers specific for the SARS-CoV-2 *N2* gene region. Digital PCR methods, in our and others' hands, are more sensitive than conventional PCR to detect SARS-CoV-2 copies in biological fluids with low viral titers [28, 29]. As shown in **Figures S2** and **1F**, determination of the viral copy number was more precise with this technique. In particular, it was possible to appreciate that also the cell line expressing the lowest ACE2 levels produced viral particles in the supernatant (e.g. 72 hours, 10 MOI), even though their amount was almost three Log_{10} lower than those produced by the 'Hi' cells under the same conditions. To confirm that these viral particles are infective, we finally exposed the kidney-derived Vero E6 cell line [30] to the supernatants of the infected cSt-Cs, followed by the determination of the fifty-percent tissue culture infective dose ($TCID_{50}$, see **Supplementary information**). Results of titration confirmed dPCR quantifications, showing a dose- and time-related increased infectivity above baseline recorded for ACE2 'Hi' cellular supernatant and a gradual decrease of viral load in the supernatant of ACE2 'Lo' cells (**Figure S3**). Taken together, these results suggest that cSt-Cs are susceptible to infection by SARS-CoV-2 in an ACE2-dependent manner and capable to support viral replication depending on the expression level of the receptor.

3.3. Intracellular molecular bioprocessing of SARS-CoV-2 in cSt-Cs

In order to investigate SARS-CoV-2 intracellular bioprocessing, we first assessed the temporal dynamics of *E*, *N2* and *RdRP* viral transcripts in RNAs of cSt-Cs extracted cellular. In line with the previous results, clear differences were detected in the copy number of these genes in RNAs extracted from the different cell lines, with very limited number of copies/µL in 'Lo' cells at all the employed MOIs and MOI-dependent increases in 'Mid' and 'Hi' cells (**Figure 2A**). To find microscopic evidences of viral intracellular replication, we then performed immunofluorescence on ACE2 'Lo' and 'Hi' infected cells using a human anti-SARS-CoV-2 serum, together with activated fibroblasts/myofibroblasts markers alpha-smooth muscle actin (αSMA) and/or Collagen-1 (Col1). Confocal microscopy imaging showed a very little proportion of 'Lo' cells exhibiting a SARS-CoV-2 labeling clearly above background fluorescence level observed in control cells (**Figure 2B**). By contrast, the number of 'Hi' cells labeled with the serum was markedly higher (**Figure 2C**). Infected cells exhibited an intense staining with an anti-SARS-CoV-2 human serum (Figure **2D, E**) and possible swelling of the endoplasmic reticulum (ER) associated with intense viral production (**Figure 2D**)[31], or the formation of a reticulo-vesicular ER network supporting SARS-CoV-2 replication[32]. It was also interesting to observe that when cells exhibiting SARS-CoV-2 staining were found in contact with non-infected cells (**Figure 2F**), viral particles appeared to transit from the positive cell to the surrounding negative cells (see inset in **Figure 2F**). This suggests that SARS-CoV-2 may transfer from infected to uninfected cSt-Cs by direct cell- to-cell transfer, the so-called 'virological synapse', one of the modalities of viral intercellular propagation inside tissues[33].

3.4 Ultrastructural evidences of SARS-CoV-2 packaging and cytotoxicity in cSt-Cs

To substantiate further the presence of the virus in cSt-Cs and reveal signs of cytotoxicity, we performed ultrastructural analysis using transmission electron microscopy (TEM). The ultrastructural features of the infected cells exhibited clear differences from those of non-infected cells (Compare **panel b** in **Figure 3A** with **panel c** in **Figure 3B**). Namely, infected cells exhibited swelling of the rough endoplasmic reticulum (rER) with ribosomes frequently dissociated from the ER structure. This observation has been previously associated with high level of viral production[31], and again suggests the formation of reticulo-vesicular ER networks supporting SARS-coronavirus replication[32], as also shown in **Figure 2D.** Cells exposed to the virus also showed bigger multilamellar bodies (LB) visible in the cell cytoplasm compared to control cells (compare **panel c** in **Figure 3A** with **panel b** in **Figure 3B**). SARS-CoV-2 virions were detected, alone or

in clusters, predominantly in intracellular compartments (i.e. vacuoles) (**Figure 3B panels c, d** and **3C panel c**), as previously shown in different cultured cell lines and lung cells of infected patients[34]. Finally, cells exhibiting a high number of viral particles outside intracellular structures were found (**Figure 3C panels a, b**) and clear signs of s of degeneration, such as cytoplasm condensation were also observed (**Figure 3C panels a, b, d**).

3.5. Pro-inflammatory and pro-fibrotic responses of cSt-Cs exposed to SARS-CoV-2

CSt-Cs have a central role in cardiac healing following acute injury, as they trigger the production of inflammatory cytokines and extracellular matrix remodeling enzymes necessary for the recruitment of leukocytes and activation of the innate immunity process priming myocardium repair[20]. Since SARS-CoV-2 infection causes sharp upregulation of inflammatory cytokines in target organs through infection-dependent and innate immunity signaling mediated by Toll-like receptors[35], cardiac inflammation observed in COVID-19 patients may result from a combination of the systemic 'cytokine storm' and a direct inflammatory response by cardiac-resident cells[36]. To assess this hypothesis, we tested the effects of the virus on the activation of inflammatory factors and genes potentially involved in cardiac fibrosis[16]. We therefore analyzed the expression of genes involved in innate immune response and cardiotoxicity using RNAs extracted from the three cell lines infected with 10 MOI SARS-CoV-2 for 2, 24 and 72 hours. To do this, we used low-density PCR arrays containing primers specific for tissue inflammation and fibrosis, as well as single RT-qPCR tests (see Supplementary Information for further details). As shown in **Table S4,** 17 genes out of the 168 contained in the low-density arrays were significantly over/down modulated in infected cells *vs.* the uninfected cells at the same time point. This regulation was clearly time dependent and did not reflect differences in ACE2 expression. Unsupervised clusterization of the average fold changes (**Figure 4A**) revealed a coordinated regulation of genes that were significantly more expressed at early (*HSP1, PD4, FOSL, BCL2A1, HMOX*), intermediate (*ITPR2, RND1, ZNF148*), and late (NEXN, SERPINE1, ZNF23, CCL7, FHL1, ICAM1, EGR1, STAT-1) time points, respectively. In particular, the genes that were significantly upregulated as early as at 2 hours post-infection indicate an early response of cSt-Cs to stress conditions determined by exposure to the virus. For example, *HSPH1 (hsp110)* is a heat shock protein strongly upregulated in response to coronaviruses exposure and in particular to their Envelope (E) proteins[37], while *FOSL1* is a transcription/cellular factor engaged in Interferon signaling in responses to viral infection[38]. It was remarkable to note that some of the transcripts significantly upregulated at 72 hours post-infection in response to virus

encode for, ***i)*** a membrane adhesion protein involved in cell-to-cell intercellular viral transmission (e.g. ICAM1) [39]; ***ii)*** a chemokine with potent *pro*-inflammatory effects (CCL7/MCP3) in COVID-19 [40, 41]; and ***iii)*** transcriptional regulators EGR1 and STAT1 involved, respectively, in SARS-CoV-related TGF-β1 signaling [42] and immune response in COVID-19 patients [43]. We finally investigated the regulation of mRNAs encoding for key factors involved in COVID-19 'cytokine storm' and cardiac inflammatory/fibrotic responses[1, 44, 45]. Results of single RT-qPCR tests clearly indicated that cells from the three cell lines responded to viral exposure with a time-dependent upregulation of pro-fibrotic genes *CTGF*, *ACTA2*, *Col1A* and *Col3A* and of inflammatory cytokines *IL-1β* and *CCL2* (*MCP1*) and, to a lower extent, *IL-6* mRNAs irrespective of ACE2 expression levels (**Figure 2B, C**). Together, these results highlight an additional cardiac pathogenesis mechanism by SARS-CoV-2 independent of ACE2 expression, consisting of substantial upregulation of genes involved in response to viral infection, intercellular virus transmission and related to innate immunity signaling and fibrotic activation.

4. Discussion

Experimental evidences have shown the susceptibility of cells expressing ACE2 receptor to direct infection by SARS-CoV-2 with implications for the multi-organ disease characterizing the COVID-19 pandemic outbreak. This includes endothelial[13], kidney and urogenital tract cells[46], enterocytes[47], and a variety of human iPSCs-derived cell types[48], including cardiac myocytes[16]. As of today, despite the numerous reports showing extensive cardiac damages consequent to infection[49] and the presence of the virus in myocardial biopsies[6, 50], there is still uncertainty about the underlying mechanisms[36]. As outlined in various cardiology-oriented reviews on COVID-19 pathophysiology[1, 2], the heart could be affected by cumulative effects of the cytokine storm elicited by innate immunity activation[35], as well as of *in situ* cytopathic effect determined by direct infection and replication of the virus in the myocardium[6, 50, 51].

In the present study, we provide the proof-of-concept that human myocardial stromal cells are susceptible to infection and permissive for intracellular replication of SARS-CoV-2. We also show that viral infectivity and productivity are strictly related to the expression level of the ACE2 receptor, thus confirming the influence of variations in the expression of this receptor, observed in different individuals, on the different responses to SARS-CoV-2 infection, as reported elsewhere[11]. Interestingly, the expression of ACE2 in stromal cells seemed not to be associated with anti-hypertensive therapy taken by donors of the cells (**Table S1**), thus excluding a correlation

between the susceptibility of the cells to infection and the known modulation of the receptor determined by regulators of the Renin-Angiotensin System, as discussed recently[52].

In our experiments, we constantly observed the presence of cells that did not exhibit SARS-CoV-2 staining nor cytopathic effects, even among those with 'Hi' ACE2, even at 72 hours post-infection (**Figure 2).** (**Figure 2F).** While this may reflect an inefficient viral replication in stromal cells (such as demonstrated recently for endothelial cells[14]) , it may also reflect a heterogeneous expression levels of ACE2 co-receptors[53]. Finally, our high-resolution confocal images (**Figure 2F**) also suggest the possibility of direct transmission of the virus via cell-to-cell contacts, a modality of intracellular transmission similar to that observed for other viruses, the viral synapses[33].

Our study suggests a second potential pathogenic mechanism that may be independent of direct penetration and replication of SARS-CoV-2 in cSt-Cs. Indeed, exposure to the virus was able *per se* to elicit inflammatory and pro-fibrotic responses in cSt-Cs independently of the expression of ACE2. This evidence is supported by the transcriptomic data presented in **Figure 4**, where we show a similar time-dependent trend in up/down-regulation of genes related to inflammation and fibrosis. In this regard, we hypothesize that cells exposed to the virus could mount an innate immune response by activating the nuclear factor-κB (NF-κB) pathway via the interaction of the viral Spike protein with Toll-like receptors (TLRs) [54, 55], leading to upregulation of IL6 and other pro-inflammatory cytokines such as IL1, IL2, TNF-α and Interferon (IFN)-γ, as well as pro-fibrotic genes.

Taken together, these data suggest that the variability of SARS-CoV-2 infection and spreading modality observed in the cardiac stroma may contribute to the puzzling scenario of COVID-19 cardiac complications. In particular, based on the data of the present report, we hypothesize that SARS-CoV-2 might contribute to myocardial damage with potentially cumulative effects of ***i)*** an intra-myocardial cytopathic effects due to viral replication in the stromal component directly connected to ACE2 expression levels and, ***ii)*** an ACE2-independent innate immunity response boosting myocardial inflammation and fibrosis[45]. Given the prevalently hypothesis-generating nature of our investigation, it is impossible at the moment to determine whether one of these two modalities, or both of them are prevalent in cardiac injury observed in COVID-19 patients.

Study limitations

The present work was conducted using cells derived with the cardiosphere method[23], one of the procedures used historically to obtain cells with mesenchymal-like characteristics from the human heart[27]. Since in our

experiments, cells were expanded from cellular outgrowths of right atrial appendage fragments, and through several culture passages, a potential limitation may be the selection of specific cellular phenotypes, thus determining an overall under-representation of the various stromal cells/fibroblasts subtypes present in the heart, as recently demonstrated[56].

A second limitation of our study is the reduced sample size and the lack of specific functional studies (e.g. loss of function) allowing to correlate directly the function of ACE2 receptor with viral entry and intracellular virus packaging inside cSt-Cs.

Caution should be finally adopted in extending our findings to the situation encountered in COVID-19 patients, where still today there is a heated debate about the direct *vs.* the indirect effects of SARS-CoV-2 on cardiac inflammation and fibrosis, including the occurrence of actual myocarditis[57]. In this regard, future studies using cells derived from various districts of the human heart, e.g. atrial *vs.* ventricular fibroblasts, or combining multiple cell types, e.g. cardiac fibroblasts and iPSC-derived cardiomyocytes (which also susceptible to infection[16]) in tissue constructs/organoids exposed to the virus, should be performed to address this important point.

Funding

This work has been financed by a Grant from Regione Lombardia (POR FESR 2014-2020-LINEA 2A COVID-grant no. 1850333) granted to M.P. and A.A. M.P. and A.A. are supported by Institutional grants (Ricerca Corrente, 5 per 1000) issued by the Italian Ministry of Health. A.A. was supported also by COVID-2020-12371817 and COVID-2020-12371675 program grants from the Italian Ministry of Health.

Competing Interests

The authors declare no competing interests.

Authors Contribution

AA, GG, PS, RN, SF, GB and PC performed experiments. FC, CC, GS, MRC and MA provided materials. AA, VM, MP, GIC, PP and MP supervised experiments. AA and MP provided funding. AA, GG and MP conceived the experiments. AA and MP wrote the paper.

Data Sharing Statement

The data contained in the present study will be available upon written request to the corresponding author

References

1. Akhmerov A, Marban E. COVID-19 and the Heart. *Circ Res* 2020;**126**:1443-1455.
2. Libby P. The Heart in COVID19: Primary Target or Secondary Bystander? *JACC Basic to translational science* 2020;10.1016/j.jacbts.2020.04.001:440.
3. Huang C, Wang Y, Li X, Ren L, Zhao J, Hu Y, Zhang L, Fan G, Xu J, Gu X, Cheng Z, Yu T, Xia J, Wei Y, Wu W, Xie X, Yin W, Li H, Liu M, Xiao Y, Gao H, Guo L, Xie J, Wang G, Jiang R, Gao Z, Jin Q, Wang J, Cao B. Clinical features of patients infected with 2019 novel coronavirus in Wuhan, China. *Lancet* 2020;**395**:497-506.
4. Guo T, Fan Y, Chen M, Wu X, Zhang L, He T, Wang H, Wan J, Wang X, Lu Z. Cardiovascular Implications of Fatal Outcomes of Patients With Coronavirus Disease 2019 (COVID-19). *JAMA Cardiology* 2020;**5**:811.
5. Baldi E, Sechi GM, Mare C, Canevari F, Brancaglione A, Primi R, Klersy C, Palo A, Contri E, Ronchi V, Beretta G, Reali F, Parogni P, Facchin F, Rizzi U, Bussi D, Ruggeri S, Oltrona Visconti L, Savastano S. COVID-19 kills at home: the close relationship between the epidemic and the increase of out-of-hospital cardiac arrests. *Eur Heart J* 2020;10.1093/eurheartj/ehaa508.
6. Tavazzi G, Pellegrini C, Maurelli M, Belliato M, Sciutti F, Bottazzi A, Sepe PA, Resasco T, Camporotondo R, Bruno R, Baldanti F, Paolucci S, Pelenghi S, Iotti GA, Mojoli F, Arbustini E. Myocardial localization of coronavirus in COVID-19 cardiogenic shock. *Eur J Heart Fail* 2020;**22**:911-915.
7. Sala S, Peretto G, Gramegna M, Palmisano A, Villatore A, Vignale D, De Cobelli F, Tresoldi M, Cappelletti AM, Basso C, Godino C, Esposito A. Acute myocarditis presenting as a reverse Tako-Tsubo syndrome in a patient with SARS-CoV-2 respiratory infection. *European Heart Journal* 2020;10.1093/eurheartj/ehaa286.
8. Dong N, Cai J, Zhou Y, Liu J, Li F. End-stage Heart Failure with COVID-19: Strong Evidence of Myocardial Injury by 2019-nCoV. *JACC Heart failure* 2020;10.1016/j.jchf.2020.04.001.
9. Escher F, Pietsch H, Aleshcheva G, Bock T, Baumeier C, Elsaesser A, Wenzel P, Hamm C, Westenfeld R, Schultheiss M, Gross U, Morawietz L, Schultheiss HP. Detection of viral SARS-CoV-2 genomes and histopathological changes in endomyocardial biopsies. *ESC Heart Failure* 2020;**7**:2440-2447.
10. Zou X, Chen K, Zou J, Han P, Hao J, Han Z. Single-cell RNA-seq data analysis on the receptor ACE2 expression reveals the potential risk of different human organs vulnerable to 2019-nCoV infection. *Frontiers of Medicine* 2020;10.1007/s11684-020-0754-0.
11. Nicin L, Abplanalp WT, Mellentin H, Kattih B, Tombor L, John D, Schmitto JD, Heineke J, Emrich F, Arsalan M, Holubec T, Walther T, Zeiher AM, Dimmeler S. Cell type-specific expression of the putative SARS-CoV-2 receptor ACE2 in human hearts. *Eur Heart J* 2020;**41**:1804-1806.
12. Wang Q, Zhang Y, Wu L, Niu S, Song C, Zhang Z, Lu G, Qiao C, Hu Y, Yuen KY, Zhou H, Yan J, Qi J. Structural and Functional Basis of SARS-CoV-2 Entry by Using Human ACE2. *Cell* 2020;10.1016/j.cell.2020.03.045.
13. Varga Z, Flammer AJ, Steiger P, Haberecker M, Andermatt R, Zinkernagel AS, Mehra MR, Schuepbach RA, Ruschitzka F, Moch H. Endothelial cell infection and endotheliitis in COVID-19. *Lancet* 2020;10.1016/S0140-6736(20)30937-5.
14. McCracken IR, Saginc G, He L, Huseynov A, Daniels A, Fletcher S, Peghaire C, Kalna V, Andaloussi-Mäe M, Muhl L, Craig NM, Griffiths SJ, Haas JG, Tait-Burkard C, Lendahl U, Birdsey GM, Betsholtz C, Noseda M, Baker AH, Randi AM. Lack of Evidence of ACE2 Expression and Replicative Infection by SARSCoV-2 in Human Endothelial Cells. *Circulation* 2021;**0**.
15. Sharma A, Garcia G, Arumugaswami V, Svendsen CN. Human iPSC-Derived Cardiomyocytes are Susceptible to SARS-CoV-2 Infection. *bioRxiv* 2020;10.1101/2020.04.21.051912:2020.2004.2021.051912.
16. Bojkova D, Wagner JUG, Shumliakivska M, Aslan GS, Saleem U, Hansen A, Luxán G, Günther S, Pham MD, Krishnan J, Harter PN, Ermel UH, Frangakis AS, Milting H, Zeiher AM, Klingel K, Cinatl J, Dendorfer A, Eschenhagen T, Tschöpe C, Ciesek S, Dimmeler S. SARS-CoV-2 infects and induces cytotoxic effects in human cardiomyocytes. *Cardiovascular Research* 2020;10.1093/cvr/cvaa267.
17. Souders CA, Bowers SL, Baudino TA. Cardiac fibroblast: the renaissance cell. *Circ Res* 2009;**105**:1164-1176.

18. Moore-Morris T, Cattaneo P, Puceat M, Evans SM. Origins of cardiac fibroblasts. *Journal of Molecular and Cellular Cardiology* 2016;**91**:1-5.
19. Frangogiannis NG. Cardiac fibrosis. *Cardiovascular Research* 2020;10.1093/cvr/cvaa324.
20. Humeres C, Frangogiannis NG. Fibroblasts in the Infarcted, Remodeling, and Failing Heart. *JACC Basic to translational science* 2019;**4**:449-467.
21. Travers JG, Kamal FA, Robbins J, Yutzey KE, Blaxall BC. Cardiac Fibrosis: The Fibroblast Awakens. *Circ Res* 2016;**118**:1021-1040.
22. Pappritz K, Savvatis K, Koschel A, Miteva K, Tschope C, Van Linthout S. Cardiac (myo)fibroblasts modulate the migration of monocyte subsets. *Scientific Reports* 2018;**8**:5575.
23. Messina E, De Angelis L, Frati G, Morrone S, Chimenti S, Fiordaliso F, Salio M, Battaglia M, Latronico MV, Coletta M, Vivarelli E, Frati L, Cossu G, Giacomello A. Isolation and expansion of adult cardiac stem cells from human and murine heart. *Circ Res* 2004;**95**:911-921.
24. Capobianchi MR, Rueca M, Messina F, Giombini E, Carletti F, Colavita F, Castilletti C, Lalle E, Bordi L, Vairo F, Nicastri E, Ippolito G, Gruber CEM, Bartolini B. Molecular characterization of SARS-CoV-2 from the first case of COVID-19 in Italy. *Clin Microbiol Infect* 2020;**26**:954-956.
25. Avanzini MA, Mura M, Percivalle E, Bastaroli F, Croce S, Valsecchi C, Lenta E, Nykjaer G, Cassaniti I, Bagnarino J, Baldanti F, Zecca M, Comoli P, Gnecchi M. Human mesenchymal stromal cells do not express ACE2 and TMPRSS2 and are not permissive to SARS-CoV-2 infection. *Stem Cells Translational Medicine* 2020;**n/a**.
26. Carlson S, Trial J, Soeller C, Entman ML. Cardiac mesenchymal stem cells contribute to scar formation after myocardial infarction. *Cardiovasc Res* 2011.
27. Smith RR, Barile L, Cho HC, Leppo MK, Hare JM, Messina E, Giacomello A, Abraham MR, Marban E. Regenerative potential of cardiosphere-derived cells expanded from percutaneous endomyocardial biopsy specimens. *Circulation* 2007;**115**:896-908.
28. Suo T, Liu X, Feng J, Guo M, Hu W, Guo D, Ullah H, Yang Y, Zhang Q, Wang X, Sajid M, Huang Z, Deng L, Chen T, Liu F, Ke X, Liu Y, Zhang Q, Liu Y, Xiong Y, Chen G, Lan K, Chen Y. ddPCR: a more sensitive and accurate tool for SARS-CoV-2 detection in low viral load specimens. *medRxiv* 2020;10.1101/2020.02.29.20029439:2020.2002.2029.20029439.
29. Poggio P, Songia P, Vavassori C, Ricci V, Banfi C, Barbieri SS, Garoffolo G, Myasoedova VA, Piacentini L, Raucci A, Scopece A, Sommariva E, Vinci MC, Carcione D, Biondi ML, Mancini ME, Formenti A, Andreini D, Assanelli EM, Agostoni P, Camera M, Colombo GI, Pesce M. Digital PCR for high sensitivity viral detection in false-negative SARS-CoV-2 patients. *Scientific Reports* 2021;**11**:4310.
30. Keyaerts E, Vijgen L, Maes P, Neyts J, Van Ranst M. Growth kinetics of SARS-coronavirus in Vero E6 cells. *Biochem Biophys Res Commun* 2005;**329**:1147-1151.
31. Romero-Brey I, Bartenschlager R. Endoplasmic Reticulum: The Favorite Intracellular Niche for Viral Replication and Assembly. *Viruses* 2016;**8**:160.
32. Knoops K, Kikkert M, Worm SH, Zevenhoven-Dobbe JC, van der Meer Y, Koster AJ, Mommaas AM, Snijder EJ. SARS-coronavirus replication is supported by a reticulovesicular network of modified endoplasmic reticulum. *PLoS Biol* 2008;**6**:e226.
33. Zhong P, Agosto LM, Munro JB, Mothes W. Cell-to-cell transmission of viruses. *Curr Opin Virol* 2013;**3**:44-50.
34. Nardacci R, Colavita F, Castilletti C, Lapa D, Matusali G, Meschi S, Nonno FD, Colombo D, Capobianchi MR, Zumla A, Ippolito G, Piacentini M, Falasca L. SARS-CoV-2 cytopathogenesis in cultured cells and in COVID-19 autoptic lung, evidences of lipid involvement. *Research Square* 2020;10.21203/rs.3.rs-39274/v1.
35. Sallenave JM, Guillot L. Innate Immune Signaling and Proteolytic Pathways in the Resolution or Exacerbation of SARS-CoV-2 in Covid-19: Key Therapeutic Targets? *Frontiers in immunology* 2020;**11**:1229.
36. Guzik TJ, Mohiddin SA, Dimarco A, Patel V, Savvatis K, Marelli-Berg FM, Madhur MS, Tomaszewski M, Maffia P, D'Acquisto F, Nicklin SA, Marian AJ, Nosalski R, Murray EC, Guzik B, Berry C, Touyz RM, Kreutz R, Wang DW, Bhella D, Sagliocco O, Crea F, Thomson EC, McInnes IB. COVID-19 and the cardiovascular system: implications for risk assessment, diagnosis, and treatment options. *Cardiovasc Res* 2020;**116**:1666-1687.

37. DeDiego ML, Nieto-Torres JL, Jimenez-Guardeno JM, Regla-Nava JA, Alvarez E, Oliveros JC, Zhao J, Fett C, Perlman S, Enjuanes L. Severe acute respiratory syndrome coronavirus envelope protein regulates cell stress response and apoptosis. *PLoS Pathog* 2011;**7**:e1002315.
38. Cai B, Wu J, Yu X, Su XZ, Wang RF. FOSL1 Inhibits Type I Interferon Responses to Malaria and Viral Infections by Blocking TBK1 and TRAF3/TRIF Interactions. *mBio* 2017;**8**:e02161-02116.
39. Bracq L, Xie M, Benichou S, Bouchet J. Mechanisms for Cell-to-Cell Transmission of HIV-1. *Frontiers in immunology* 2018;**9**:260.
40. Yang Y, Shen C, Li J, Yuan J, Wei J, Huang F, Wang F, Li G, Li Y, Xing L, Peng L, Yang M, Cao M, Zheng H, Wu W, Zou R, Li D, Xu Z, Wang H, Zhang M, Zhang Z, Gao GF, Jiang C, Liu L, Liu Y. Plasma IP-10 and MCP-3 levels are highly associated with disease severity and predict the progression of COVID-19. *The Journal of allergy and clinical immunology* 2020;**146**:119-127 e114.
41. Vaninov N. In the eye of the COVID-19 cytokine storm. *Nature reviews Immunology* 2020;**20**:277.
42. Li SW, Wang CY, Jou YJ, Yang TC, Huang SH, Wan L, Lin YJ, Lin CW. SARS coronavirus papain-like protease induces Egr-1-dependent up-regulation of TGF-beta1 via ROS/p38 MAPK/STAT3 pathway. *Sci Rep* 2016;**6**:25754.
43. Zhu L, Yang P, Zhao Y, Zhuang Z, Wang Z, Song R, Zhang J, Liu C, Gao Q, Xu Q, Wei X, Sun HX, Ye B, Wu Y, Zhang N, Lei G, Yu L, Yan J, Diao G, Meng F, Bai C, Mao P, Yu Y, Wang M, Yuan Y, Deng Q, Li Z, Huang Y, Hu G, Liu Y, Wang X, Xu Z, Liu P, Bi Y, Shi Y, Zhang S, Chen Z, Wang J, Xu X, Wu G, Wang FS, Gao GF, Liu L, Liu WJ. Single-Cell Sequencing of Peripheral Mononuclear Cells Reveals Distinct Immune Response Landscapes of COVID-19 and Influenza Patients. *Immunity* 2020;10.1016/j.immuni.2020.07.009.
44. Adao R, Guzik TJ. Inside the heart of COVID-19. *Cardiovasc Res* 2020;**116**:e59-e61.
45. Ammirati E, Wang DW. SARS-CoV-2 inflames the heart. The importance of awareness of myocardial injury in COVID-19 patients. *Int J Cardiol* 2020;**311**:122-123.
46. Wang S, Zhou X, Zhang T, Wang Z. The need for urogenital tract monitoring in COVID-19. *Nature reviews Urology* 2020;**17**:314-315.
47. Lamers MM, Beumer J, van der Vaart J, Knoops K, Puschhof J, Breugem TI, Ravelli RBG, Paul van Schayck J, Mykytyn AZ, Duimel HQ, van Donselaar E, Riesebosch S, Kuijpers HJH, Schippers D, van de Wetering WJ, de Graaf M, Koopmans M, Cuppen E, Peters PJ, Haagmans BL, Clevers H. SARS-CoV-2 productively infects human gut enterocytes. *Science* 2020;10.1126/science.abc1669:eabc1669.
48. Yang L, Han Y, Nilsson-Payant BE, Gupta V, Wang P, Duan X, Tang X, Zhu J, Zhao Z, Jaffre F, Zhang T, Kim TW, Harschnitz O, Redmond D, Houghton S, Liu C, Naji A, Ciceri G, Guttikonda S, Bram Y, Nguyen DT, Cioffi M, Chandar V, Hoagland DA, Huang Y, Xiang J, Wang H, Lyden D, Borczuk A, Chen HJ, Studer L, Pan FC, Ho DD, tenOever BR, Evans T, Schwartz RE, Chen S. A Human Pluripotent Stem Cell-based Platform to Study SARS-CoV-2 Tropism and Model Virus Infection in Human Cells and Organoids. *Cell Stem Cell* 2020;**27**:125-136 e127.
49. Giustino G, Croft LB, Stefanini GG, Bragato R, Silbiger JJ, Vicenzi M, Danilov T, Kukar N, Shaban N, Kini A, Camaj A, Bienstock SW, Rashed ER, Rahman K, Oates CP, Buckley S, Elbaum LS, Arkonac D, Fiter R, Singh R, Li E, Razuk V, Robinson SE, Miller M, Bier B, Donghi V, Pisaniello M, Mantovani R, Pinto G, Rota I, Baggio S, Chiarito M, Fazzari F, Cusmano I, Curzi M, Ro R, Malick W, Kamran M, Kohli-Seth R, Bassily-Marcus AM, Neibart E, Md GS, Perk G, Mancini D, Reddy VY, Pinney SP, Dangas G, Blasi F, Sharma SK, Mehran R, Condorelli G, Stone GW, Fuster V, Lerakis S, Goldman ME. Characterization of Myocardial Injury in Patients With COVID-19. *Journal of the American College of Cardiology* 2020;**76**:2043-2055.
50. Wenzel P, Kopp S, Gobel S, Jansen T, Geyer M, Hahn F, Kreitner KF, Escher F, Schultheiss HP, Munzel T. Evidence of SARS-CoV-2 mRNA in endomyocardial biopsies of patients with clinically suspected myocarditis tested negative for COVID-19 in nasopharyngeal swab. *Cardiovasc Res* 2020;10.1093/cvr/cvaa160.
51. Thum T. SARS-CoV-2 receptor ACE2 expression in the human heart: cause of a post-pandemic wave of heart failure? *Eur Heart J* 2020;**41**:1807-1809.
52. Gul R, Kim U-H, Alfadda AA. Renin-angiotensin system at the interface of COVID-19 infection. *European Journal of Pharmacology* 2021;**890**:173656.
53. Singh M, Bansal V, Feschotte C. A Single-Cell RNA Expression Map of Human Coronavirus Entry Factors. *Cell Reports* 2020;**32**:108175.

54. Dosch SF, Mahajan SD, Collins AR. SARS coronavirus spike protein-induced innate immune response occurs via activation of the NF-κB pathway in human monocyte macrophages in vitro. *Virus Research* 2009;**142**:19-27.
55. Brandão SCS, Ramos JdOX, Dompieri LT, Godoi ETAM, Figueiredo JL, Sarinho ESC, Chelvanambi S, Aikawa M. Is Toll-like receptor 4 involved in the severity of COVID-19 pathology in patients with cardiometabolic comorbidities? *Cytokine & Growth Factor Reviews* 2020;10.1016/j.cytogfr.2020.09.002.
56. Ruiz-Villalba A, Romero JP, Hernández SC, Vilas-Zornoza A, Fortelny N, Castro-Labrador L, San Martin-Uriz P, Lorenzo-Vivas E, García-Olloqui P, Palacio M, Gavira JJ, Bastarrika G, Janssens S, Wu M, Iglesias E, Abizanda G, de Morentin XM, Lasaga M, Planell N, Bock C, Alignani D, Medal G, Prudovsky I, Jin Y-R, Ryzhov S, Yin H, Pelacho B, Gomez-Cabrero D, Lindner V, Lara-Astiaso D, Prósper F. Single-Cell RNA Sequencing Analysis Reveals a Crucial Role for CTHRC1 (Collagen Triple Helix Repeat Containing 1) Cardiac Fibroblasts After Myocardial Infarction. *Circulation* 2020;**142**:1831-1847.
57. Van Linthout S, Klingel K, Tschöpe C. SARS-CoV-2 related myocarditis-like syndromes. Shakespeare's question: what's in a name? *EUROPEAN JOURNAL OF HEART FAILURE* 2020;**22**:922-925.

Figure Legends

Figure 1. Expression of ACE2 and response of cST-Cs to infection with SARS-CoV-2. (A) Western blot analysis of ACE2 protein expression in cST-Cs lines from 10 donors (**Table S1**). ACE2 band is colored in green with a molecular weight (MW) ~86 kDa. In red the GAPDH bands (MW 37 kDa) used for data normalization. On the right side, it is indicated the result of a linear regression analysis of protein/RNA data in the same cells, showing a highly significant data correlation. In color it is indicated the 90% confidence interval. In both panels, numbers and symbols in color indicate, respectively, the data from the 'Lo' (blue), 'Mid' (red) and 'Hi' (green) cSt-Cs. **(B)** Flow cytometry analysis of the cST-Cs with mesenchymal and endothelial markers. The FACS plots show overlapped of the antigen expression profile of the three cell lines chose for the experiments (each represented by their color code, see **Table S1**). The box-plot contains the min-max antigen expression data of the 10 cSt-Cs lines, with an indication of the three donors chosen for the experimental study represented by circles colored with the code adopted in **panel A** and **Table S1**. **(C)** Representative image of non-infected (CTRL, left panel) and SARS-CoV-2 infected 'Hi' cSt-Cs cells (1 MOI – 72 hours, center and right panels) showing swelling of the cytoplasm and release of microparticles (red arrows, center panel), and cytopathic effect characterized by cell rounding and wrinkling (yellow arrows, right panel). **(D)** Graphic representation of the mean Ct values of *Spike* and *ORF-1* viral RNAs detected in the supernatant of the cell lines exposed to different amounts of SARS-CoV-2 at the indicated time points. Although not statistically significant (ns) when compared with ANOVA followed by pairwise post-hoc tests (n=3), a trend to increase in the expression of the two genes at 24 and 72 hours *vs.* 2 hours post-infection al all the MOIs was evident. (**E**) Representation of the viral release by the three cell lines in the supernatant by plotting of *Spike* and *ORF* Ct values measured by RT-qPCR amplification revealed a time-dependent increase in viral release by ACE2 'Hi' and, at a lower extent, by 'Mid' cells. The 'Lo' cells exhibited no variations compared to the level of the baseline at 2 hours. The three graphs sets indicate the Ct values of the two viral genes detected in the culture supernatants of each cell line at each time point and MOI. **(F)** dPCR detection of *N2* SARS-CoV-2 gene in cSt-Cs culture supernatant, indicative of absolute virus copy number expressed in copy number/µL. This analysis allowed to quantify with better resolution the release of viral particles by the three lines, and in particular, that even cells with the lowest level of ACE2 expression were able to produce viral particles in little amounts (see, e.g. the 72 hours - 10 MOI time point). The three graphs sets indicate the temporal increase in the amount of SARS-CoV-2 copies detected in the culture supernatants of each cell line at each MOI.

Figure 2. Intracellular bioprocessing of SARS-CoV-2 in cSt-Cs. (A) The intracellular bioprocessing of the virus was monitored by dPCR performed on cSt-Cs cellular RNAs extracted from cells at various times post-infection. In this case, the number of copies was normalized to *RpLP0* mRNA, used as a cellular internal control. Plots indicate variations in *N2*, *E* and *RdRp* normalized copies/mL, demonstrating expression of viral RNAs inside cells, and providing an accurate estimate of the SARS-Cov-2 replication in cSt-Cs with different ACE2 expression (note the difference in the scale of the three plots in the panel). The three graphs sets indicate

the temporal increase (hours) in the viral genes detected in the RNA extracted from each cell line exposed to each SARS-CoV-2 MOI. **(B)** Four-color immunofluorescence staining of uninfected ACE2 'Lo' and 'Hi' cells with nuclear staining (DAPI), αSMA, Collagen1 and SARS-CoV-2. In these cells, the expression of the markers was similar and the background color of SARS-CoV-2 staining was minimal. **(C)** Low-power magnification of triple-color stained cSt-Cs fixed 72 hours after exposure to SARS-CoV-2. ACE2 'Lo' cells with clear viral staining were very rare (left panel). The abundance of SARS-CoV-2-stained cells was higher in ACE2'Hi' cells; these cells exhibited a typical arrangement in small clusters among uninfected cells (mid and right panels). **(D)** Low- and high-power magnification of ACE2 'Hi' cells infected with SARS-CoV-2. In the right panel, a high-power view of the zone encircled in the white square on the left. The oval structures surrounded by intense SARS-CoV-2 staining might be enlargements of the endoplasmic reticulum, one of the typical intracellular sites of virus assembly[31]. **(E)** High-power view of a cell showing αSMA^{+} stress fibers (left) and a cytoplasm densely packed with SARS-CoV-2 particles (insets). **(F)** In the panel on the left it is represented the low-power view of a cluster of cSt-Cs positive and negative for SARS-CoV-2 staining. Note in the right panel the 3D projection of a z-stacked acquisition of the region encircled in the white box in the left panel, where the boundary between the SARS-CoV-2^{+} and the SARS-CoV-2^{-} cells seems to be crossed by viral particles, indicative of possible direct cell-to-cell virus transmission.

Figure 3. Transmission electron microscopy images of ACE2-Hi cSt-Cs exposed to SARS-CoV-2. (**A**) Low and high magnification of control cSt-Cs. (**a**) Low magnification of two adjacent cells where the nuclei (N), the mitochondria, the rough endoplasmic reticulum (rER) are visible. (**b, c**) High magnification of control cells showing in better detail the rER as well as small vacuoles containing some single membrane small vesicles (V, arrows), and multilamellar bodies (LB). (**B**) Low and high power views of ultrastructural features of cSt-Cs exposed to SARS-CoV-2. (**a, c**) Low/mid magnification of cellular structures showing the presence of numerous free ribosomes (arrow in **c**) and enlargement of the rER (arrowheads in **c**). (**b, d**) magnification of the regions encircled by insets in panels **a** and **c**. It is evident the enlargement of the multilamellar bodies (LB) in panel **b** and the presence of virions in a vesicular structure connected to the rER in **d** (arrows). (**C**) Ultrastructure of a cSt-Cs (**a**) exhibiting numerous virions in the cytoplasm (**b, d**) or inside vacuoles (**c**). Note the cytoplasm condensation of the cell in panel **a,** and the typical appearance of the viral particles displaying characteristic black dots, due to the cross-sectioning of the viral nucleocapsid in **b** and **d** (arrows).

Figure 4. Innate immunity and pro-fibrotic responses in cSt-Cs exposed to SARS-CoV-2. (A) Two RT-qPCR gene arrays containing primers for amplification of 164 transcripts potentially involved in cardiotoxicity and innate immune signaling were employed to assess changes in gene expression consequent to exposure of the three cSt-Cs lines exposed to 10 MOI SARS-CoV-2. After identification of the genes significantly changed in their expression levels at 2, 24 and 72 hours post-infection with a *P*-value < 0.05 by ANOVA (**Table S4**), an unsupervised data clusterization was conducted. Results showed a coordinated time-dependent clusterization of the transcripts of the three cell lines, with groups of up and downmodulated genes at the different time points. Raw data of this experiment are represented in **Table S4**. **(B, C)** The expression

of genes typically involved in cSt-Cs pro-fibrotic activation (*CTGF, ACTA2, Col1A and Col3A*) and the SARS-CoV-2 cytokine storm (*Il-β, CCL2/MCP1, IL-6*) was finally investigated by single RT-qPCR tests on cellular RNAs at the three time points and at all the tested viral concentrations (MOI 0.1, 1, 10). As shown, expression of *pro*-fibrotic genes (**B**) exhibited variability in relationship to the viral dose used in infection experiments, especially for *Col1A* and *CTGF*. In contrast, expression of genes encoding for the pro-inflammatory cytokines (**C**) was more consistently upregulated in the three lines above the level of uninfected cells already at 24 hours of expression. Upregulation of transcription of these genes appeared independent of the level of ACE2 expression, as evidenced by overlapping the values of the gene expression fold changes in each cell line (color coded as in **Fig 1A** and **Table S1**) to the bar graphs indicating the average and the standard error of the data. In both panels * indicates $P < 0.05$ statistical significance by one-way ANOVA analysis (repeated measures) calculated on the ΔCt values for each gene at each viral concentration used for the infected *vs.* uninfected cells (n=3) at 24 and 72 hours post-infection.

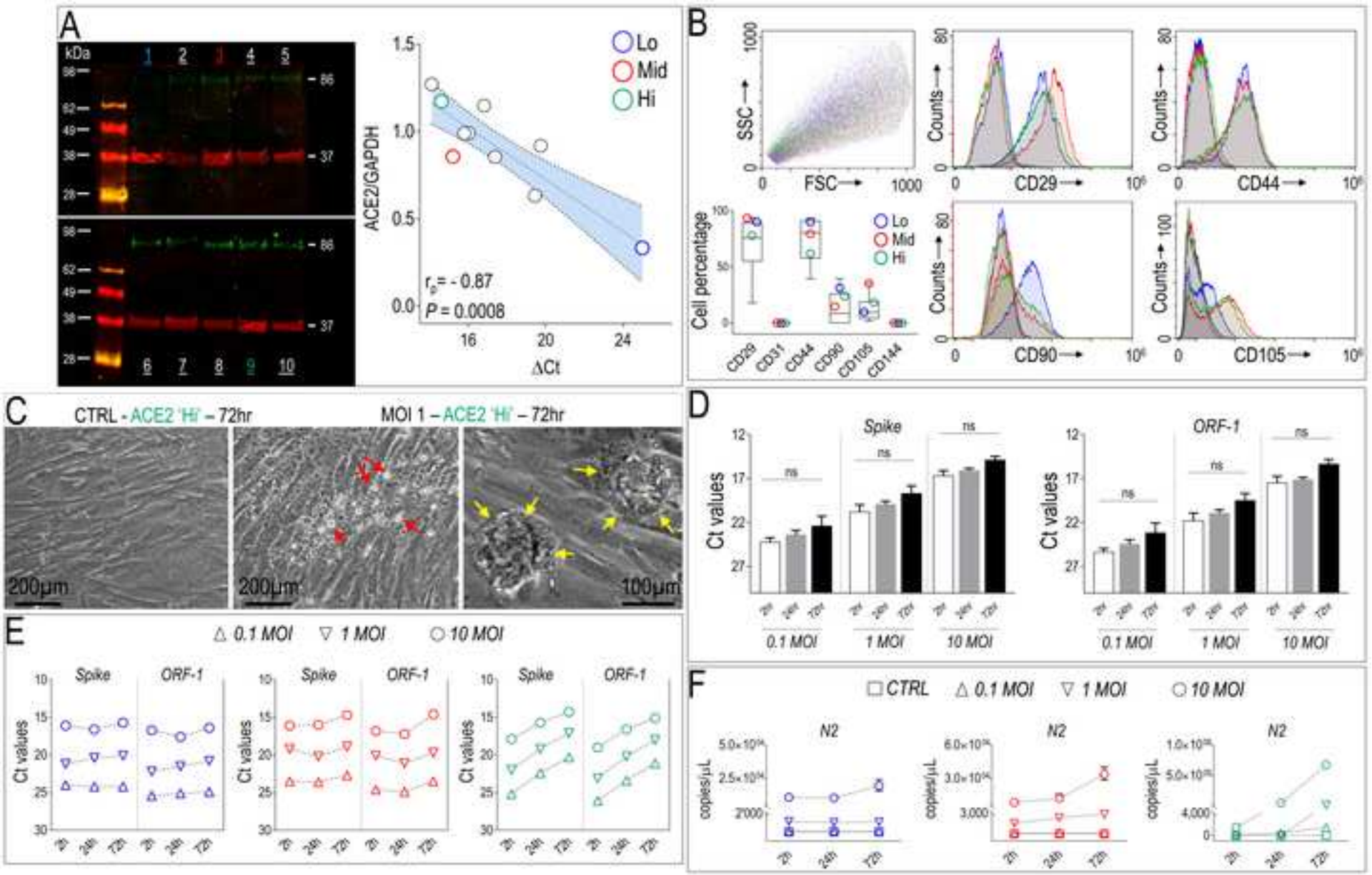
A
kDa
1 2 3 4 5
86
62
49
38
28
37
6 7 8 9 10
ACE2/GAPDH
ΔCt
Lo
Mid
Hi
r_s = - 0.87
P = 0.0008
B
SSC
FSC
Counts
CD29
CD44
CD90
CD105
Cell percentage
CD29 CD31 CD44 CD90 CD105 CD144
C
CTRL - ACE2 'Hi' – 72hr
MOI 1 – ACE2 'Hi' – 72hr
200µm
100µm
D
Spike
ORF-1
Ct values
ns
0.1 MOI
1 MOI
10 MOI
E
△ 0.1 MOI ▽ 1 MOI ○ 10 MOI
F
□ CTRL △ 0.1 MOI ▽ 1 MOI ○ 10 MOI
N2
copies/µL

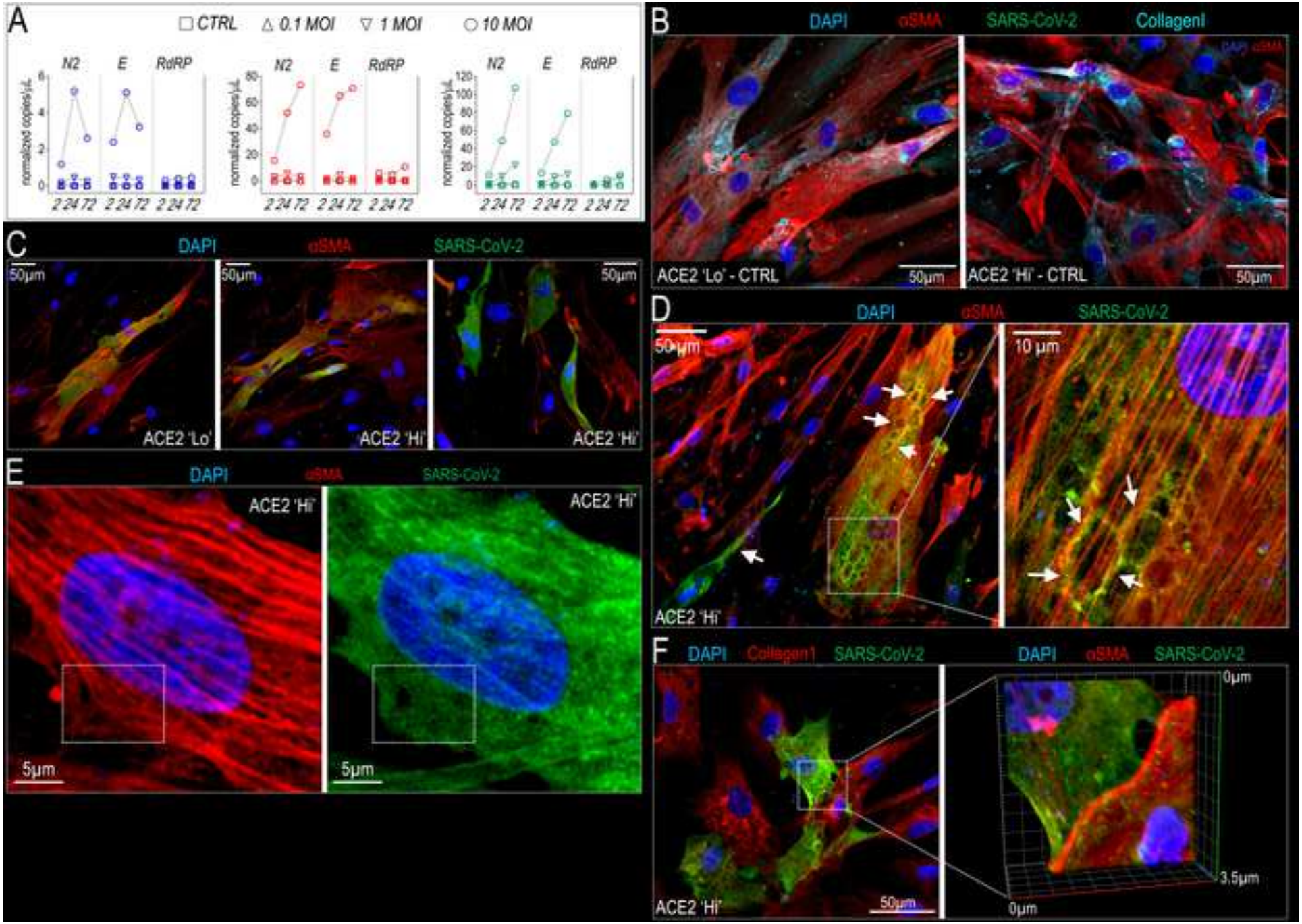
A
CTRL
0.1 MOI
1 MOI
10 MOI
N2
E
RdRP
normalized copies/µL
2 24 72
B
DAPI
αSMA
SARS-CoV-2
Collagen I
ACE2 'Lo' - CTRL
ACE2 'Hi' - CTRL
50µm
C
DAPI
αSMA
SARS-CoV-2
ACE2 'Lo'
ACE2 'Hi'
D
10 µm
E
5µm
F
Collagen1
0µm
3.5µm

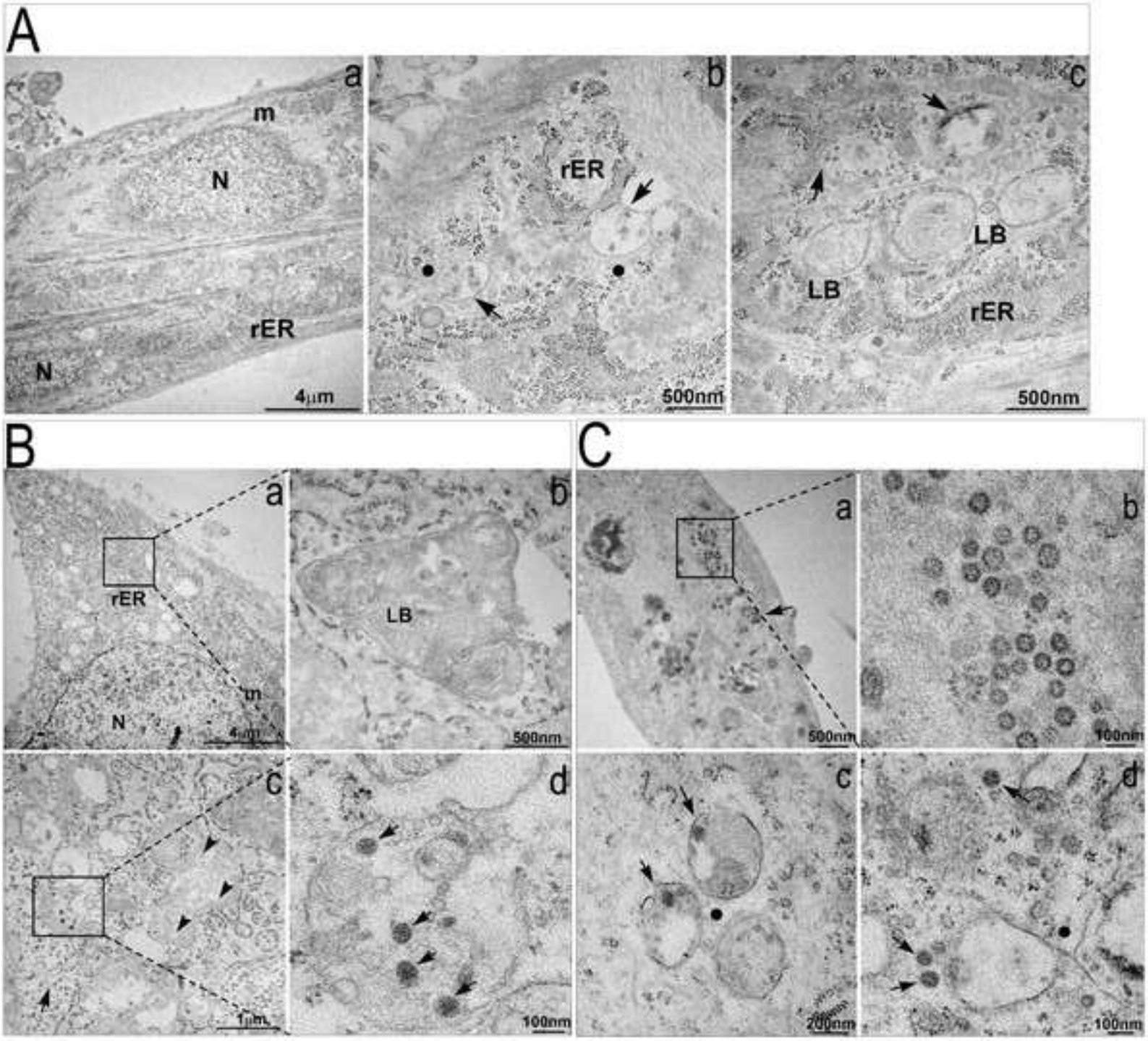
A
a
m
N
rER
N
4μm
b
rER
500nm
c
LB
LB
rER
500nm
B
a
rER
m
N
4μm
b
LB
500nm
c
1μm
d
100nm
C
a
500nm
b
100nm
c
200nm
d
100nm

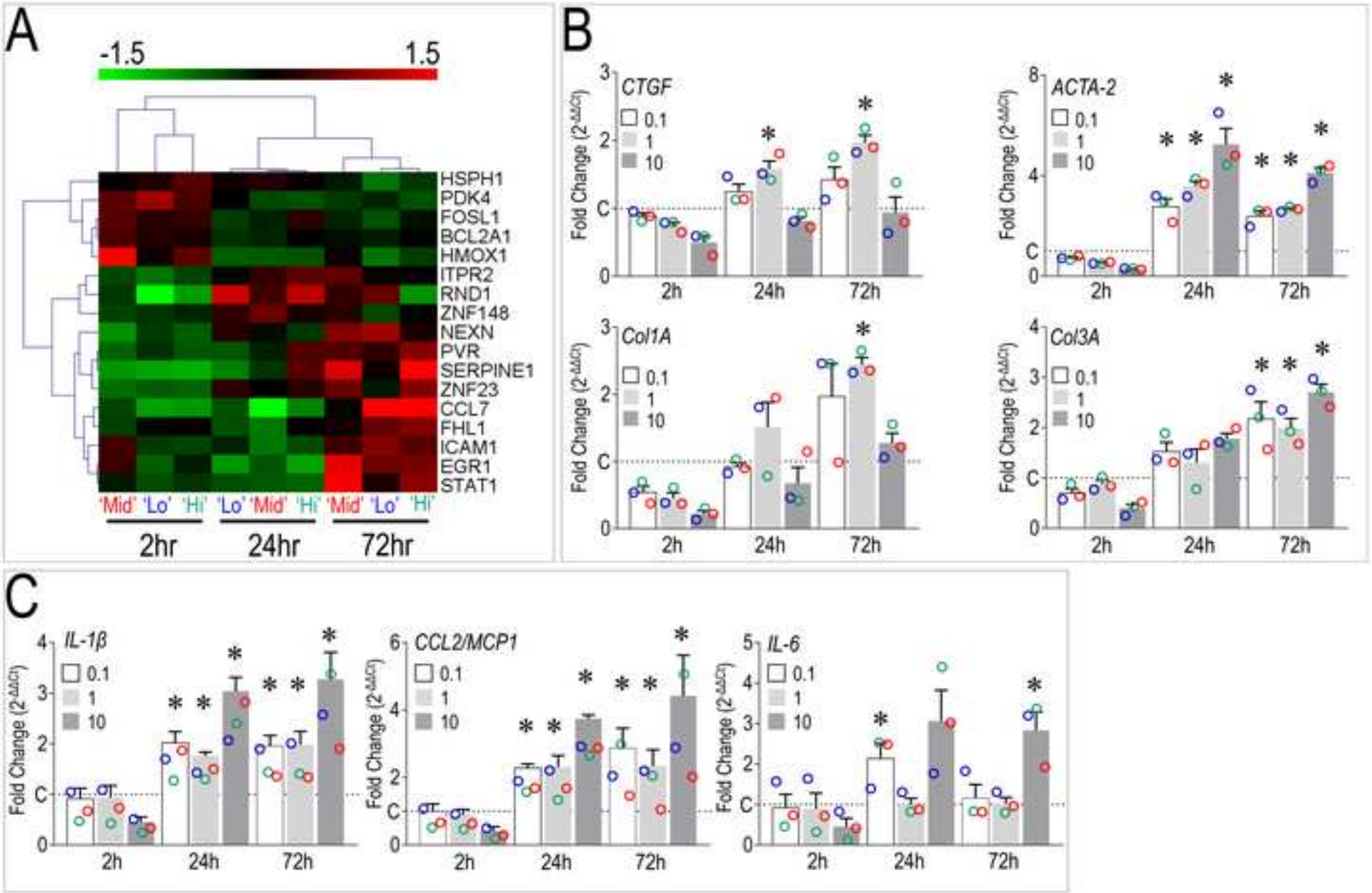
A
-1.5
1.5
HSPH1
PDK4
FOSL1
BCL2A1
HMOX1
ITPR2
RND1
ZNF148
NEXN
PVR
SERPINE1
ZNF23
CCL7
FHL1
ICAM1
EGR1
STAT1
'Mid' 'Lo' 'Hi' 'Lo' 'Mid' 'Hi' 'Mid' 'Lo' 'Hi'
2hr
24hr
72hr
B
CTGF
ACTA-2
Col1A
Col3A
0.1
1
10
Fold Change (2-ΔΔCt)
C
2h
24h
72h
C
IL-1β
CCL2/MCP1
IL-6